Percolation transition and dissipation in quantum Ising magnets

José A. Hoyos and Thomas Vojta
Department of Physics, University of Missouri-Rolla, Rolla, Missouri 65409, USA.

We study the effects of dissipation on a randomly diluted transverse-field Ising magnet close to the percolation threshold. For weak transverse fields, a novel percolation quantum phase transition separates a superparamagnetic cluster phase from an inhomogeneously ordered ferromagnetic phase. The properties of this transition are dominated by large frozen and slowly fluctuating percolation clusters. This leads to a discontinuous magnetization-field curve and exotic hysteresis phenomena as well as highly singular behavior of magnetic susceptibility and specific heat. We compare our results to the smeared transition in generic dissipative random quantum Ising magnets. We also discuss the relation to metallic quantum magnets and other experimental realizations.

In diluted quantum magnets, the combination of geometric and quantum fluctuations can lead to unconventional low-temperature properties such as singular thermodynamic quantities in quantum Griffiths phases as well as exotic scaling at the quantum phase transitions (QPTs) between magnetic and nonmagnetic ground states[1–4] (for a recent review see, e.g., Ref. 5). In many real systems, the magnetic degrees of freedom are coupled to an environment of "heat bath" modes. The dissipation caused by the bath is known to qualitatively change the properties even of a single quantum spin.[6–9].

In this Letter, we show that dissipation dramatically changes phases and phase transitions of a randomly diluted quantum Ising magnet, as is illustrated by Fig. 1. The behavior without dissipation is well understood:[10–13] Magnetic long-range order exists for dilutions p up to the lattice percolation threshold p_c as long as the transverse field h_x is below a critical field $h_c(p)$. For $p > p_c$, long-range order is impossible because the system is decomposed into noninteracting finite-size clusters. There are two QPTs, separated by a multicritical point at (p_c, h^*). The transition across $h_c(p)$ for $0 < p < p_c$ (transition (i) in Fig. 1a) falls into the generic random quantum Ising universality class and is characterized by an infinite-randomness fixed point.[1,2] The transition across p_c at $h_x < h^*$ (transition (ii) in Fig. 1a) is an unusual kind of percolation QPT.[13] The paramagnetic phase consists of two regions: a conventional gapped region for $h_x > h_c(0)$ and a gapless quantum Griffiths region for $h_x < h_c(0)$ where rare regions lead to power-law thermodynamic singularities.

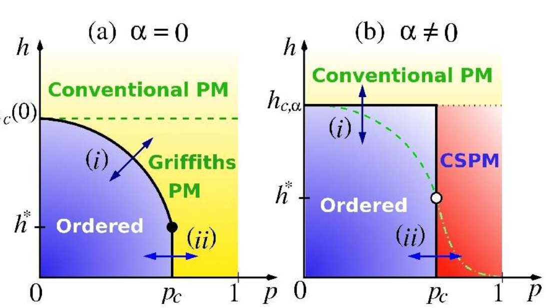

FIG. 1: Schematic ground state phase diagrams of diluted quantum Ising magnets without (a) and with (b) dissipation. CSPM is the classical superparamagnetic phase. The dashed line in (b) marks the crossover between homogeneous and inhomogeneous order in the smeared transition scenario.

In the presence of weak ohmic dissipation, the phase diagram changes qualitatively since the quantum dynamics of sufficiently large clusters freezes.[14–16] This leads to the appearance of an unusual classical superparamagnetic cluster phase. For $p > p_c$, it is stabilized down to zero temperature because different clusters are strictly decoupled. In contrast, for $p < p_c$ weakly coupled frozen rare regions align. Magnetic long-range order thus extends to the clean critical field $h_{c,\alpha}$, and the field-driven phase transition (i) is smeared.[17–19]

In this Letter, we focus on the novel percolation QPT at small fields h_x (transition (ii) in Fig. 1b). Our results can be summarized as follows: The total magnetization consists of a coherent part m_∞ and an incoherent part $m_{\rm st}$. The critical behavior of the coherent part is given by classical percolation theory $m_\infty \sim |p - p_c|^{\beta_c}$ with β_c the classical percolation exponent. Somewhat unexpectedly, $m_\infty + m_{\rm st}$ (which is measured in an infinitesimal ordering field) is *noncritical* at p_c. The interplay between the two parts leads to unusual magnetization-field hysteresis. At low temperatures T, the susceptibility has a Curie contribution from the frozen clusters that diverges as $\chi \sim |p - p_c|^{-\gamma_c}/T$ with the classical percolation exponent γ_c. Fluctuating clusters provide a subleading $1/(T \ln^2 T)$ contribution. In contrast, the low-temperature specific heat is dominated by fluctuating clusters, resulting in a logarithmic temperature dependence, $C \sim \ln^{-2}(1/T)$. The logarithmic terms in χ and C exist on both sides of p_c and their prefactors are noncritical at this point .

Our starting point is a d-dimensional ($d \geq 2$) site-diluted transverse-field Ising model[10–13]

$$H_I = -J \sum_{\langle i,j \rangle} \epsilon_i \epsilon_j \sigma_i^z \sigma_j^z - h_x \sum_i \epsilon_i \sigma_i^x \ , \qquad (1)$$

a prototypical disordered quantum magnet. The Pauli matrices σ_i^z and σ_i^x represent the spin components at site i, the exchange interaction J couples nearest neighbor sites, and the transverse field h_x controls the quantum fluctuations. Dilution is introduced via random variables ϵ_i which can take the values 0 and 1 with probabilities

p and $1-p$, respectively. We now couple each spin to a local ohmic bath of harmonic oscillators,[19,20]

$$H = H_I + \sum_{i,n}\left[\nu_{i,n} a^\dagger_{i,n} a_{i,n} + \frac{1}{2}\lambda_{i,n}\sigma^z_i (a^\dagger_{i,n} + a_{i,n})\right], \quad (2)$$

where $a_{i,n}$ and $a^\dagger_{i,n}$ are the annihilation and creation operators of the n-th oscillator coupled to spin i; $\nu_{i,n}$ is its frequency, and $\lambda_{i,n}$ is the coupling constant. All baths have the same spectral function $\mathcal{E}(\omega) = \pi \sum_n \lambda^2_{i,n}\delta(\omega - \nu_{i,n})/\nu_{i,n} = 2\pi\alpha\omega e^{-\omega/\omega_c}$ with α the dimensionless dissipation strength and ω_c the cutoff energy. Such local ohmic dissipation can be realized in good approximation in magnetic nanoparticles in an insulating host.[21] It also applies to resistively shunted SQUIDs[6] and qualitatively (possibly with a different spectral density $\mathcal{E}(\omega)$) to molecular magnets weakly coupled to nuclear spins[22] (see, e.g., the spin-1/2 molecular complex V_{15}, Ref. 23).

Let us start by considering a single percolation cluster of s occupied sites. Without dissipation, and for small transverse fields, $h_x \ll h_{c,\alpha} \sim J$, its lowest two energy levels correspond to the states of a single effective Ising spin with a moment proportional to s in an effective transverse field (tunneling matrix element) Δ_s. For large s, Δ_s can be estimated in s-th order of perturbation theory to be $h_x e^{-Bs}$, with B a constant of order $\ln(J/h_x)$.[13] All other levels are separated by energies of order J and can thus be neglected for the low-energy physics. This means the cluster tunnels coherently between *up* and *down* with a tunneling frequency Δ_s.

The effects of the heat bath on the cluster can be worked out in 2nd order perturbation theory in h_x. We find that the effective spin of the cluster feels a single ohmic bath with dissipation strength $As\alpha$ because the number of oscillators coupling to the cluster is proportional to s.[24] Here, A is an h_x-dependent constant which we suppress as it can be absorbed in the cluster moment. Analogous results have been obtained for the dissipative random quantum Ising chain[19] and itinerant Ising magnets.[15] Each percolation cluster thus behaves like an ohmic spin-boson model:[6,7] For strong dissipation, $s\alpha > \alpha_c \approx 1$[37], the cluster is in the localized phase, i.e., the renormalized tunneling matrix element $\Delta_{R,s}$ vanishes, and the magnetization is frozen in one of the directions. Clusters with $s\alpha < 1$ are in the delocalized phase, i.e., they still tunnel, but with a greatly reduced frequency. For $s\alpha \ll 1$ it can be estimated by adiabatic renormalization[6],

$$\Delta_{R,s} \sim \Delta_s \left(\Delta_s/\omega_c\right)^{\alpha_s/(1-\alpha_s)} = h_x \exp\left[-bs/(1-s\alpha)\right] , \quad (3)$$

with the constant $b = B + \alpha \ln(\omega_c/h_x)$. The QPT at $s\alpha = 1$ is of Kosterlitz-Thouless[25] type, analogous to the transition in the classical $1/r^2$ Ising chain.[26,27] Here, $\Delta_{R,s}$ plays the role of the classical correlation length. Therefore, the functional form (3) remains valid as long as $1 - s\alpha > \Delta_s/\omega_c$. However, very close to the transition, $1 - s\alpha < \Delta_s/\omega_c$, eq. (3) has to be replaced by[28]

$$\Delta_{R,s} \sim h_x \exp\left(-b's/\sqrt{1-s\alpha}\right) . \quad (4)$$

These results allows us to determine the phase diagram, Fig. 1b, for fixed small dissipation strength α. For $h_x > h_{c,\alpha}$, our system is a conventional gapped quantum paramagnet for all p because not even the clean bulk system orders. For $h_x < h_{c,\alpha}$ and $p > p_c$, the system is decomposed into finite-size percolation clusters. The largest of these clusters are frozen and behave like classical Ising magnets while the smaller ones fluctuate. The system is thus in a classical superparamagnetic cluster phase. For $p < p_c$, ferromagnetic long-range order exists on the infinite percolation cluster. The ferromagnetic phase extends up to the clean critical field $h_{c,\alpha}$ for all $p < p_c$. This is a manifestation of the smeared transition scenario:[17] The infinite percolation cluster contains, with small probability, large impurity-free regions that freeze close to $h_{c,\alpha}$. Due to their coupling to the rest of the infinite cluster they induce a highly inhomogeneous but coherent magnetization already for transverse fields close to $h_{c,\alpha}$. For smaller transverse fields there will be a crossover to homogeneous order on the infinite cluster (see the dashed line in Fig. 1b).

To study the percolation QPT, we need the distribution of cluster sizes as a function of dilution p. According to percolation theory,[29] the number n_s of occupied clusters of size s per lattice site obeys the scaling form

$$n_s\left(t\right) = s^{-\tau_c} f\left(t s^{\sigma_c}\right). \quad (5)$$

Here $t = p - p_c$, and τ_c and σ_c are classical percolation exponents[38]. The scaling function $f(x)$ is analytic for small x and has a single maximum at some $x_{\max} > 0$. For large $|x|$, it drops off rapidly

$$f(x) \sim \begin{cases} \exp\left(-(c_1 x)^{1/\sigma_c}\right) & (\text{for } x > 0), \\ \exp\left(-(c_2 x)^{(1-1/d)/\sigma_c}\right) & (\text{for } x < 0), \end{cases} \quad (6)$$

where c_1 and c_2 are constants of order unity. In addition, for $p < p_c$, there is an infinite cluster containing a fraction $P_\infty \sim |p - p_c|^{\beta_c}$ of all sites. All classical percolation exponents are determined by τ_c and σ_c including the correlation length exponent $\nu_c = (\tau_c - 1)/(d\sigma_c)$, the order parameter exponent $\beta_c = (\tau_c - 2)/\sigma_c$, and the susceptibility exponent $\gamma_c = (3 - \tau_c)/\sigma_c$.

The low-energy density of states (DOS) $\rho_{\rm dy}(\epsilon)$ of the dynamic clusters ($s\alpha < 1$) can be determined by combining the single-cluster results (3) and (4) with the cluster size distribution (5) via $\rho_{\rm dy}(\epsilon) = \sum_{s<s_c} n_s\, \delta(\epsilon - \Delta_{R,s})$. Inserting (3) for $\Delta_{R,s}$ yields

$$\rho_{\rm dy}(\epsilon) = n_{s(\epsilon)}\, b / \left[\epsilon \left(b + \alpha \ln(h_x/\epsilon)\right)^2\right] , \quad (7)$$

where $n_{s(\epsilon)}$ is the density of clusters of size $s(\epsilon) = \ln(h_x/\epsilon)/[b + \alpha\ln(h_x/\epsilon)]$. Eq. (7) contains the full crossover between quantum Griffiths behavior at higher energies and damping-dominated behavior at low energies. For $\epsilon > \epsilon_{\rm cross} = h_x e^{-b/\alpha}$, the DOS simplifies to a

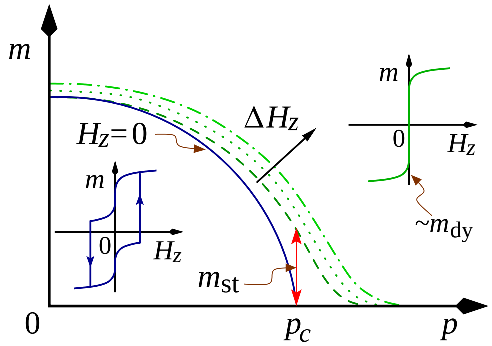

FIG. 2: Zero-temperature magnetization as a function of dilution p for different ordering fields H_z. The solid line is the coherent magnetization at $H_z = 0$ (infinite cluster only). The dashed line is for an infinitesimal field. The insets show the singular field dependence of m below and above p_c.

power-law form, $\rho_{\rm dy}(\epsilon) \sim \epsilon^{c/b-1}$, characteristic of quantum Griffiths behavior.[3] In contrast, for $\epsilon < \epsilon_{\rm cross}$, the energy dependence is even more singular,

$$\rho_{\rm dy}(\epsilon) \sim n_{s_c}/[\epsilon \ln^{\phi}(h_x/\epsilon)] , \qquad (8)$$

with $\phi = 2$. At very low energies, in the asymptotic region of the Kosterlitz-Thouless transition, $\Delta_{R,s}$ is given by (4) which leads to $\phi = 3$. The functional form (8) of the low-energy DOS is the same on both sides of the percolation threshold since it is caused by clusters of *finite size* $s \approx s_c = 1/\alpha$. Moreover, the prefactor is noncritical at p_c because the cluster size distribution n_s is an analytic function of p for any finite s.

We now discuss the physics at the percolation transition in small transverse fields ($h_x \ll h_{c,\alpha}$), starting with the total magnetization m. We have to distinguish the contributions m_{dy} from dynamic clusters, m_{st} from frozen finite-size clusters, and m_∞ from the infinite percolation cluster, if any. For zero ordering field H_z in z-direction, m_{dy} vanishes, because the dynamic clusters are in symmetric superpositions of the *up* and *down* states. The frozen finite-size clusters individually have a nonzero magnetization, but it sums up to $m_{st} = 0$ because they do not align coherently for $H_z = 0$. The only coherent contribution to the total magnetization is m_∞. Since the infinite cluster is long-range ordered for small transverse field h_x, its magnetization is proportional to the number P_∞ of sites in the infinite cluster, giving

$$m = m_\infty \sim P_\infty(p) \sim \left\{ \begin{array}{ll} |p-p_c|^{\beta_c} & (\text{for } p<p_c), \\ 0 & (\text{for } p>p_c), \end{array} \right. \qquad (9)$$

(solid line in Fig. 2). The magnetization critical exponent is given by its classical lattice percolation value β_c

The zero-temperature response of the magnetization to a small ordering field H_z is highly singular. Frozen finite-size clusters align parallel to the field already for infinitesimal H_z, leading to a jump in $m(H_z)$ at $H_z = 0$. The magnitude of the jump is given by $m_{\rm st} \sim \sum_{s>s_c} n_s$. At the percolation threshold, $m_{\rm st}$ is approximately given by $(1-p_c)s_c^{2-\tau_c}$, and it is exponentially small for both $p \to 0$ and $p \to 1$. Somewhat surprisingly, the total magnetization in an infinitesimal field, given by $m_\infty + m_{\rm st}$, is analytic (i.e., noncritical) at $p = p_c$ (see dashed line in Fig. 2). This follows from the fact that only clusters with sizes below s_c are *not* polarized. Since the cluster size distribution is analytic for any finite s, their total size is analytic at p_c, and consequently $m_\infty + m_{\rm st}$ must be analytic, too. To estimate the contribution $m_{\rm dy}$ of the dynamic clusters to the magnetization, we integrate the magnetization of a single cluster, $H_z s^2(\epsilon)/(H_z^2 s^2(\epsilon) + \epsilon^2)^{1/2}$ over the DOS given in (7). For small fields $H_z < \epsilon_{\rm cross}/s_c$, the main contribution comes from clusters with lowest energies and sizes close to s_c, resulting in a highly singular dependence of $m_{\rm dy}$ on the ordering field, $m_{\rm dy} \sim n_{s_c}/\ln^{\phi-1}(h_x/H_z)$ for $H_z \to 0$. For higher fields, we find a crossover to quantum Griffiths behavior of the form $m_{\rm dy} \sim H_z^{c/b}$.

As a consequence, our system displays unusual hysteresis (insets of Fig. 2). For $p < p_c$, the long-range ordered infinite cluster contributes a conventional single-domain hysteresis loop. Finite-size frozen clusters do not show hysteresis, for arbitrarily small H_z, they relax with a nonzero rate.[6] Thus, they contribute jumps in m at $H_z = 0$. The dynamic clusters add logarithmic singularities at $H_z = 0$. For $p > p_c$, there is no infinite cluster, but the jump at $H_z = 0$ as well as the logarithmic singularity survive. The above picture is valid for adiabatically slow sweeps of the ordering field H_z. If H_z is changed at a finite rate, the largest clusters will fall out of equilibrium which leads to very interesting time-dependent hysteresis phenomena that will be reported elsewhere.[24]

The low-temperature susceptibility is dominated by the contribution $\chi_{\rm st}$ of the static clusters, each of which has a Curie susceptibility of the form s^2/T. Summing over all static clusters gives

$$\chi_{\rm st} \sim \sum_{s>s_c} n_s s^2/T \sim |p-p_c|^{-\gamma_c}/T \qquad (10)$$

close to the percolation threshold. For $p \to 0$ and $p \to 1$, the prefactor of the Curie term vanishes exponentially. To determine the subleading contribution $\chi_{\rm dy}$ of the dynamic clusters, we integrate the susceptibility $[s^2(\epsilon)\tanh(\epsilon/T)]/\epsilon$ of a single cluster over the DOS (7). For $T < \epsilon_{\rm cross}$, $\chi_{\rm dy}$ is dominated by the clusters with lowest energies and sizes close to s_c, giving $\chi_{\rm dy} \sim n_{s_c}/[T \ln^{\phi-1}(h_x/T)]$. For temperatures above $\epsilon_{\rm cross}$, damping becomes unimportant and $\chi_{\rm dy}$ takes the quantum Griffiths form $\chi_{\rm dy} \sim T^{c/b-1}$.

Finally, we consider the heat capacity which is dominated by finite size clusters, the infinite cluster does not contribute for $T \ll J$. The heat capacity of a single dynamic cluster with gap ϵ is *not* equal to that of a two-level system, but given by $C \approx \pi\alpha s(\epsilon)T/(3\epsilon)$ for $T \ll \epsilon$ and $C \sim (\epsilon/T)^{2-2s(\epsilon)\alpha}$ for $T \gg \epsilon$.[30] Integrating over the DOS (8) gives $C_{\rm dy} \sim n_{s_c}/\ln^{\phi-1}(h_x/T)$. The frozen clusters contribute a term of the same functional form,

$C_{\rm st} \sim n_{s_c}/\ln^{\phi-1}(h_x/T)$. For $T > \epsilon_{\rm cross}$, the logarithmic temperature dependence is replaced by the quantum Griffiths behavior $C \sim T^{c/b}$.

To summarize, we have have shown that the diluted quantum Ising model with ohmic dissipation undergoes a novel percolation QPT. Observables dominated by the frozen clusters, such as total magnetization and susceptibility, show classical percolation critical behavior. For these quantities our analysis is asymptotically exact. Observables dominated by the fluctuating clusters, such as the heat capacity, are *noncritical* across the percolation threshold but display singular temperature dependencies (that can be expressed in terms of the low-energy properties of the ohmic spin-boson model). In the remaining paragraphs we put our results into broader perspective.

In contrast to the generic transition for $p < p_c$ (transition (i) in Fig. 1b), our percolation transition (transition (ii) in Fig. 1b) is not smeared by the mechanism of Ref. 17 because different percolation clusters are not coupled. Instead, the frozen clusters make an *incoherent* contribution to the magnetization. Deviations from a pure percolation scenario can change this. If tails in the interaction couple (even very weakly) different frozen clusters, they align coherently, and the smeared transition scenario is restored. However, for a rapidly decaying interaction, the smearing of the percolation transition becomes important only at very low energies.

In addition to the experimental examples mentioned after (2), our dissipative quantum Ising model is related to itinerant Ising magnets where the damping is due to the electrons. Integrating out the bath modes in (2) leads to a model in the same universality class as Hertz'[31] field theory for the itinerant antiferromagnetic transition.[20,32] Thus, local ohmic dissipation correctly captures the *leading* effects of the damping of the magnetic modes in itinerant magnets. It should be emphasized, however, that itinerant magnets contain extra complications such as long-range RKKY interactions, making a pure percolation scenario very unlikely. In Ref. 16, a theory similar to our description of the classical superparamagnetic phase was suggested as an explanation of the unusual thermodynamics[33] of heavy fermion compounds. Such a theory can be expected to hold above the smeared phase transition.[17] Moreover, the importance of the dissipation in these systems is currently controversial.[34–36]

Other possible applications include two-level atoms in diluted optical lattices coupled to an electromagnetic field, random arrays of tunneling defects in solids or, in the future, many coupled qubits in a noisy environment.

We acknowledge discussions with H. Rieger, J. Schmalian, and M. Vojta. This work has been supported by the NSF under grant no. DMR-0339147, and by Research Corporation.

1. D. S. Fisher, Phys. Rev. Lett. **69**, 534 (1992).
2. D. S. Fisher, Phys. Rev. B **51**, 6411 (1995).
3. M. Thill and D. A. Huse, Physica A **214**, 321 (1995).
4. A. P. Young and H. Rieger, Phys. Rev. B **53**, 8486 (1996).
5. T. Vojta, J. Phys. A **39**, R143 (2006).
6. A. J. Leggett, S. Chakravarty, A. T. Dorsey, M. P. A. Fisher, A. Garg, and W. Zwerger, Rev. Mod. Phys. **59**, 1 (1987).
7. U. Weiss, *Quantum dissipative systems* (World Scientific, Singapore, 1993).
8. A. C. Hewson, *The Kondo Problem to Heavy Fermions* (Cambridge University Press, Cambridge, 1993).
9. M. Vojta, Phil. Mag. **86**, 1807 (2006).
10. A. B. Harris, J. Phys. C **7**, 3082 (1974).
11. R. Stinchcombe, J. Phys. C **14**, L263 (1981).
12. R. R. dos Santos, J. Phys. C **15**, 3141 (1982).
13. T. Senthil and S. Sachdev, Phys. Rev. Lett. **77**, 5292 (1996).
14. A. J. Millis, D. K. Morr, and J. Schmalian, Phys. Rev. Lett. **87**, 167202 (2001).
15. A. J. Millis, D. K. Morr, and J. Schmalian, Phys. Rev. B **66**, 174433 (2002).
16. A. H. Castro Neto and B. A. Jones, Phys. Rev. B **62**, 14975 (2000).
17. T. Vojta, Phys. Rev. Lett. **90**, 107202 (2003).
18. T. Vojta, J. Phys. A **36**, 10921 (2003).
19. G. Schehr and H. Rieger, Phys. Rev. Lett. **96**, 227201 (2006).
20. L. F. Cugliandolo, G. S. Lozano, and H. Lozza, Phys. Rev. B **71**, 224421 (2005).
21. W. Wernsdorfer, Adv. Chem. Phys. **118**, 99 (2001).
22. N. V. Prokofev and P. C. E. Stamp, Rep. Progr. Phys. **63**, 669 (2000).
23. I. Chiorescu, W. Wernsdorfer, A. Müller, H. Bögge, and B. Barbara, Phys. Rev. Lett. **84**, 3454 (2000).
24. J. A. Hoyos and T. Vojta, unpublished.
25. J. M. Kosterlitz and D. J. Thouless, J. Phys. C **6**, 1181 (1973).
26. D. J. Thouless, Phys. Rev. **187**, 732 (1969).
27. J. Cardy, J. Phys. A **14**, 1407 (1981).
28. J. M. Kosterlitz, J. Phys. C **7**, 1046 (1974).
29. D. Stauffer and A. Aharony, *Introduction to Percolation Theory* (CRC Press, Boca Raton, 1991).
30. T. A. Costi and G. Zarand, Phys. Rev. B **59**, 12398 (1999).
31. J. Hertz, Phys. Rev. B **14**, 1165 (1976).
32. P. Werner, K. Völker, M. Troyer, and S. Chakravarty, Phys. Rev. Lett. **94**, 047201 (2005).
33. G. Stewart, Rev. Mod. Phys. **73**, 797 (2001).
34. A. H. Castro Neto and B. A. Jones, Europhys. Lett. **71**, 790 (2005).
35. A. J. Millis, D. K. Morr, and J. Schmalian, Europhys. Lett. **72**, 1052 (2005).
36. A. H. Castro Neto and B. A. Jones, Europhys. Lett. **72**, 1054 (2005).

37. The value $\alpha_c = 1$ is the result for $\Delta_s/\omega_c \to 0$. For finite Δ_s, α_c will be larger than one. We will neglect this difference as it is of no importance for our calculations.
38. Classical percolation exponents carry a subscript c.